LONG WAVES AND ARTIFICIAL NEURAL NETWORKS

López, M.[1], Veigas, M.[1], López, I.[1], Astariz, S.[1] and Iglesias, G.[2]

Disturbances to load and unload operations caused by excessive vessel movements are a recurrent problem at the Exterior Port of Ferrol (NW Spain), where a new container terminal will be inaugurated soon. This work not only sheds light on the nature and behaviour of long waves at this port, but also investigates their influence on the vessel movements and proposes a method based on Artificial Neural Networks (ANNs) to determinate their energy levels. For this purpose, the sea level oscillations in the port area and the movements of a bulk carrier at berth were measured during winter-spring 2011. The results reveal the occurrence of resonant episodes in the basin and a varying behaviour of the long wave energy across the spectrum. The long waves inside the port basin can be classified into three frequency bands: LF (Low Frequency), VLF (Very Low Frequency) and ULF (Ultra Low Frequency). The LF band exhibits a high correlation with the offshore swell energy and is associated with the so-called infragravity waves. In addition, the joint analysis of long waves and vessel movements reveals a strong correlation between the movements in the horizontal plane (sway, surge and yaw) with the wave energy and, more importantly, with the LF band energy. Proved the relevance of the long waves—and, particularly, LF oscillations—to cargo handling operations, a ANN-based method to estimate the infragravity energy levels in the basin was successfully trained, validated and tested.

Keywords: long waves; infragravity waves; artificial neural networks; artificial intelligence

1. INTRODUCTION

The Port of Ferrol is located in the Ria of Ferrol (NW Spain), one of the estuaries facing the Atlantic Ocean that compose the Artabrian Gulf. Two lobes connected by a long narrow channel compose this ria, which is accessible through the Point Coitelada and Cape Prioriño Chico. Due to the strategic situation sheltered by the estuary, the port was exclusively established in the inner basin until recently. This so-called Interior Port received over the past decades continuous traffics of merchant, fishery and military ships, as well as sailing boats. However, the reduced lower water level at the entrance channel limits the access of the current vessels of largest sizes.

In 2001, the Port of Ferrol began a development and expansion stage with the aim of becoming one of the most important gateways in the northwest of the Iberian Peninsula. Four years later, the major upgrade was completed: a deep-water terminal—the Exterior Port—was established at the outer basin with the construction of a 1070 m breakwater across the estuary mouth. With a quay length of 1400 m dredged at −20 m, these new facilities are intended for vessels up to Capesize. In addition, a new milestone will be reached soon with the commissioning of a container terminal able to receive the Malaccamax container ships with a capacity of 18,000 TEU.

However, this historical stage of the port is being threatened by frequent disturbances to port operations. Since the Exterior Port was put into operation, large movements of vessels at berth have been reported by the Ferrol-San Cibrao Port Authority (López et al., 2012). These movements have slow loading and unloading of bulk carriers and, sometimes, even lead to the breaking of their mooring lines (López and Iglesias, 2014). Furthermore, container ships are known to be particularly restrictive with regard to ship motions and, hence, the future terminal could be affected to a greater extent. Given that modern maritime transport systems require fast cargo handling operations without delays, this situation constitute the major drawback for the Port of Ferrol and, particularly, for its future container terminal.

Until recently, the nature of these disturbances remained unknown. Discarded the actions of wind and tidal currents as feasible causes, waves appeared to be the most likely explanation for such large vessel movements. Among them, short waves or swell can induce motion in ships; nonetheless, the long waves have been related with the disturbances to vessel operations many times (Rabinovich, 2009; Sakakibara and Kubo, 2008; Candella, 2009). Long waves have periods above those of wind waves or swell, which can lead to resonant episodes known as seiches. During these episodes, the vertical displacements of the mass of water increase and induce large horizontal displacements that disturb port operations (Morison and Imberger, 1992; Okihiro and Guza, 1996). Previous works have described long waves at ports and coasts all over the world, along with their forcing mechanisms. One of the most common factors are the atmospheric processes associated to the passage of cold fronts,

[1] University of Santiago de Compostela, GICEMA, Campus Univ. s/n, 27002, Lugo, Spain
[2] School of Marine Science and Engineering, University of Plymouth, Drake Circus, Plymouth PL4 8AA, UK

squalls, storms, tornados, etc (e.g. Candella, 2009). In addition, since the phenomenon of surf-beat was originally reported by Munk (1949), the nonlinear interaction of swell has been largely related to the generation of long waves, which are also called 'infragravity waves' (e.g. Okihiro and Guza, 1996; Kovalev et al., 1991). However, a wide variety of mechanisms can generate long waves, such as: landslides (Cecioni and Bellotti, 2010), seisms (Wilson, 1972), tides (e.g. Giese et al., 1990) or jet-like currents, among others.

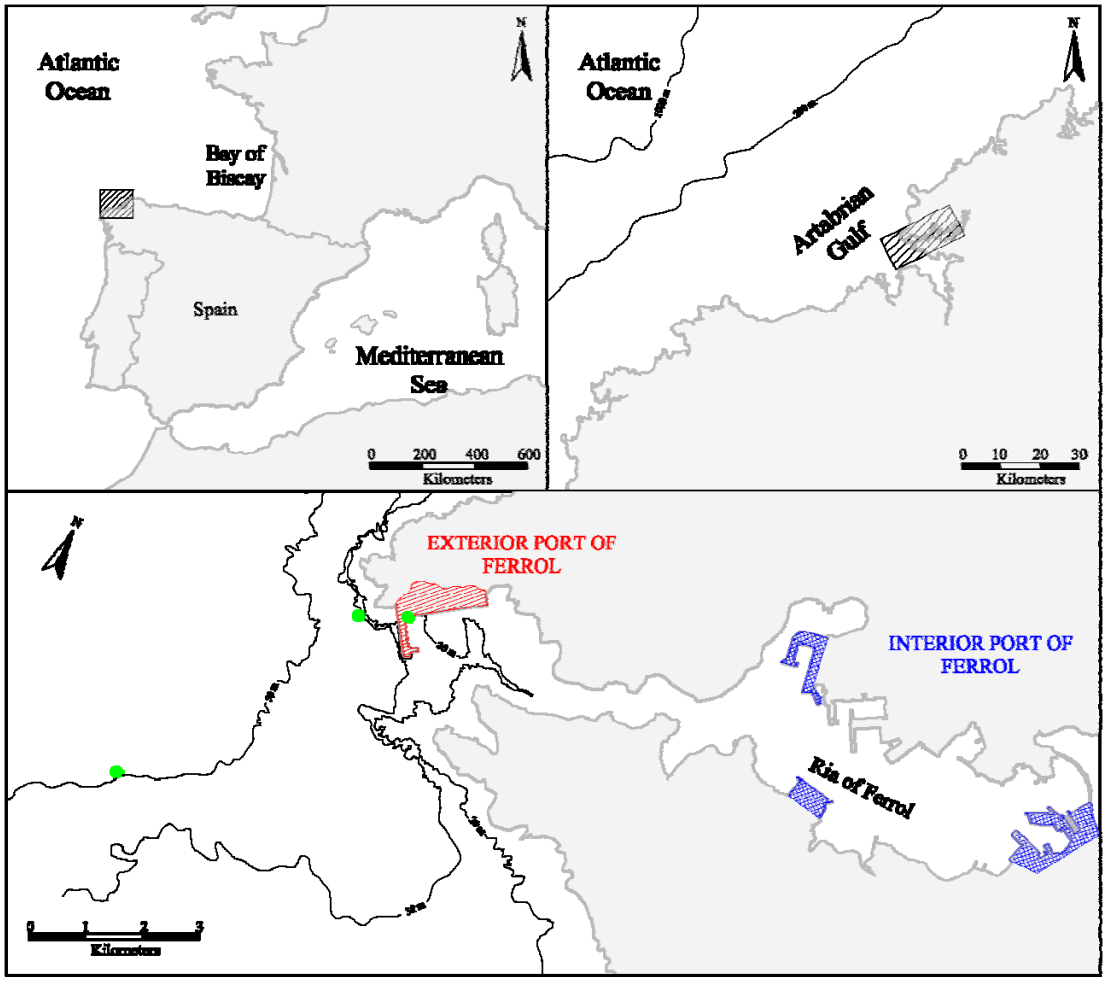

Figure 1. Location of the Exterior Port of Ferrol. The port areas (blue and red) and the positions of the sensors deployed in the field campaign are marked (green dots).

The acceptable swell conditions for safe operations at berth are listed in national and international publications and standards (e.g. Elzinga et al., 1992; PIANC, 1995). However, equivalent thresholds for long waves are unknown. The first step to solving the problem at the Exterior Port of Ferrol is to determinate the extent to which long waves are behind the disturbances to cargo handling operations. Then, once clarified their role, their nature must be also identified and their effects quantified in order to introduce mitigation alternatives. In addition, since wave and agitation database have a limited duration, methodologies to predict the long wave parameters are of major interest.

This paper is structured as follows. In Section 2, the field data used in the work are presented, including: sea level measurements and time series of vessel movements. In addition, the main techniques applied are commented. In Section 3, the long wave climate at the Port and the movements of a vessel are characterized. In addition, the results of training, validating and testing an ANN model to determinate the significant long wave height are shown. Finally, in Section 4, the conclusions of the work are drawn.

2. MATERIAL AND METHODS

2.1. Sea level measurements

A field measurement campaign was performed at the Exterior Port of Ferrol between 9 February and 14 April 2011. Two bottom-mounted pressure sensors were deployed to measure long waves outside and inside the port basin. One was located very close to the breakwater to avoid nodal lines. Another was located outside the harbour, about 700 m off the breakwater and in a water depth of 26 m. Additional sea level data were also obtained from a permanent RADAR tide gauge station, installed on the quay wall. The sampling rate was 0.5 Hz for all the time series.

Before carrying out the any analysis, the time series were inspected to detect gaps and spikes and corrected by means of linear interpolation (Goring, 2008). Then, the tidal time series was reconstructed and subtracted from the observations to obtain the non-tidal residual (Pawlowicz et al., 2002). Finally, the components with frequencies below 0.122 mHz were filtered with an Infinite Impulse Response (IIR) Butterworth high pass filter.

2.2. Vessel movements

The movements of a bulk carrier berthed at port were recorded between 19th and 21st February 2011. The characteristics of the ship were: length overall, 289 m; beam, 45 m; maximum draft, 18 m; 169,168 Deadweight Tonnage (DWT); and 86,192 Gross Registered Tonnage (GRT). Five robotic stations, with laser distance meter and 0.5 Hz sampling rate, were deployed to measure the displacements of the vessel. Then, the time series, z(t),were obtained for each Degrees Of Freedom (DOF): heave, sway, surge, yaw, pitch and roll.

A time-domain analysis was made to characterize each movement with a significant motion amplitude, $Z_{1/3}$, computed as the average of the third of the largest motions within a record. A peak to peak criterion was applied to identify each individual motion, except in the case of sway, for which the zero-peak criterion was use (Elzinga et al., 1992).

2.2. Spectral analysis

Spectral techniques, including the Fast Fourier Transform (FFT) and the Short Time Fourier Transform (STFT), were applied. The short wave conditions were characterized through the following parameters: the peak period, T_p (the inverse of the frequency for which the spectral power density is maximum), and the significant wave height, H_s, computed as:

$$H_s = 4\sqrt{m_0} \tag{1}$$

where m_0 is the zeroth spectral moment, which can be obtained from:

$$m_n = \int_0^\infty f^n S(f)df \ , \tag{2}$$

where n is the order of the spectral moment and $S(f)$ is the spectral power density distribution.

The energy of the long waves was characterized, by analogy with short waves, using the 'significant long wave height' (e.g. Bellotti and Franco, 2011; Bowers, 1992; González-Marco et al., 2008; Melito et al., 2007). This parameter, H_x, represents the energy of a given frequency band of the spectrum and is calculated by replacing in Eq. (1) m_0 by m_x, which has the following expression:

$$m_x = \int_{f_-}^{f_+} S(f)df \ , \tag{3}$$

where f_- and f_+ are the lower and upper bounds of a given frequency band x, respectively.

The Short-Time Fourier Transform (STFT) localizes a signal by modulating it with a window function, and then computes the Fourier transform and has the following expression for a continuous time case:

$$X(\tau,\omega) = \int_{-\infty}^{\infty} x(t)\omega(t-\tau)e^{-j\omega t}dt \tag{4}$$

where $X(\tau,\omega)$ is essentially the Fourier Transform of $x(t)\omega(t-\tau)$; $x(t)$ is the time series to be transformed; and $\omega(t)$ is a rectangular window function.

2.3. Artificial Neural Networks

The type of Artificial Neural Networks (ANNs) used in this work is known as multilayer feedforward. They have a layered structure, consisting of an input layer, hidden layers and an output layer, through which the input signal propagates in a forward direction with no transmission between neurons of the same layer. The transfer or activation function of each neuron determines the output as a function of the input to the neuron. The learning algorithm employed was the back-propagation

(Johansson et al., 1992), which is a gradient-descent technique that minimizes the error by adjusting the weights in an iterative procedure. In addition, Bayesian regularization was used to prevent overfitting, which minimizes a linear combination of squared errors and weights, and modifies the linear combination so that the trained network has good generalization qualities.

To define the best performing neural topology, a number of network topologies with different number of layers and neurons per layer are initially defined, trained and validated. A cross-validation method of the *k*-fold subtype is applied for this purpose (López and Iglesias, 2013). The optimum topology selected is that one that minimizes the validation error. An estimation of the real error committed by this net can be obtained by leaving out a random data set at the beginning of the training-validation process (this set represents 'unknown' data), then the outputs for this set are computed with the already trained and validated net and the results compared with the expected test values.

3. RESULTS

3.1. Long waves

An analysis was carried out to distinguish between oscillations forced by swell and those driven by other mechanisms. The values of the determination coefficient, R^2, between the swell energy outside the port (computed as the square of H_s) and the energy across the long wave spectrum were computed (Figure 2). Based on the results, three frequency bands can be distinguished: Ultra Low Frequency ($f < 0.7$ mHz), Very Low Frequency (0.7 mHz $< f <$ 2.5 mHz) and Low Frequency ($f > 2.5$ mHz). The ULF band is negligibly determined by the swell ($R^2 < 0.2$). The LF band seems to be swell-driven as evidenced by the high values of the determination coefficient ($R^2 > 0.7$). As for the VLF band, it has a transition character between both bands.

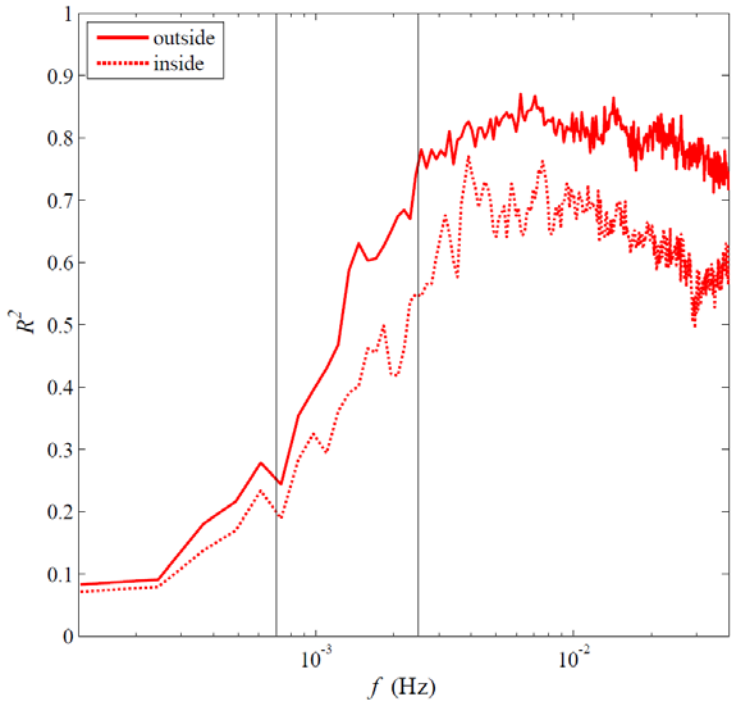

Figure 2. Coefficient of determination between $(H_s)^2$ outside the port and the power spectrum, $S(f)$, inside and outside the port for the different long wave frequencies. The frequency limits between the different frequency bands are indicated.

The spectrograms obtained with Equation (4) confirm the swell-driven character of the LF band and a resonant behaviour of the basin (Figure 3). This patter was obvious on 15th and 17th February 2011. During these episodes, the swell forced high energy levels of long waves outside the port, especially within the LF band and, in a lesser extent, within the VLF band. Inside the port, the long wave energy is amplified at different frequencies, which correspond to the natural modes of the basin.

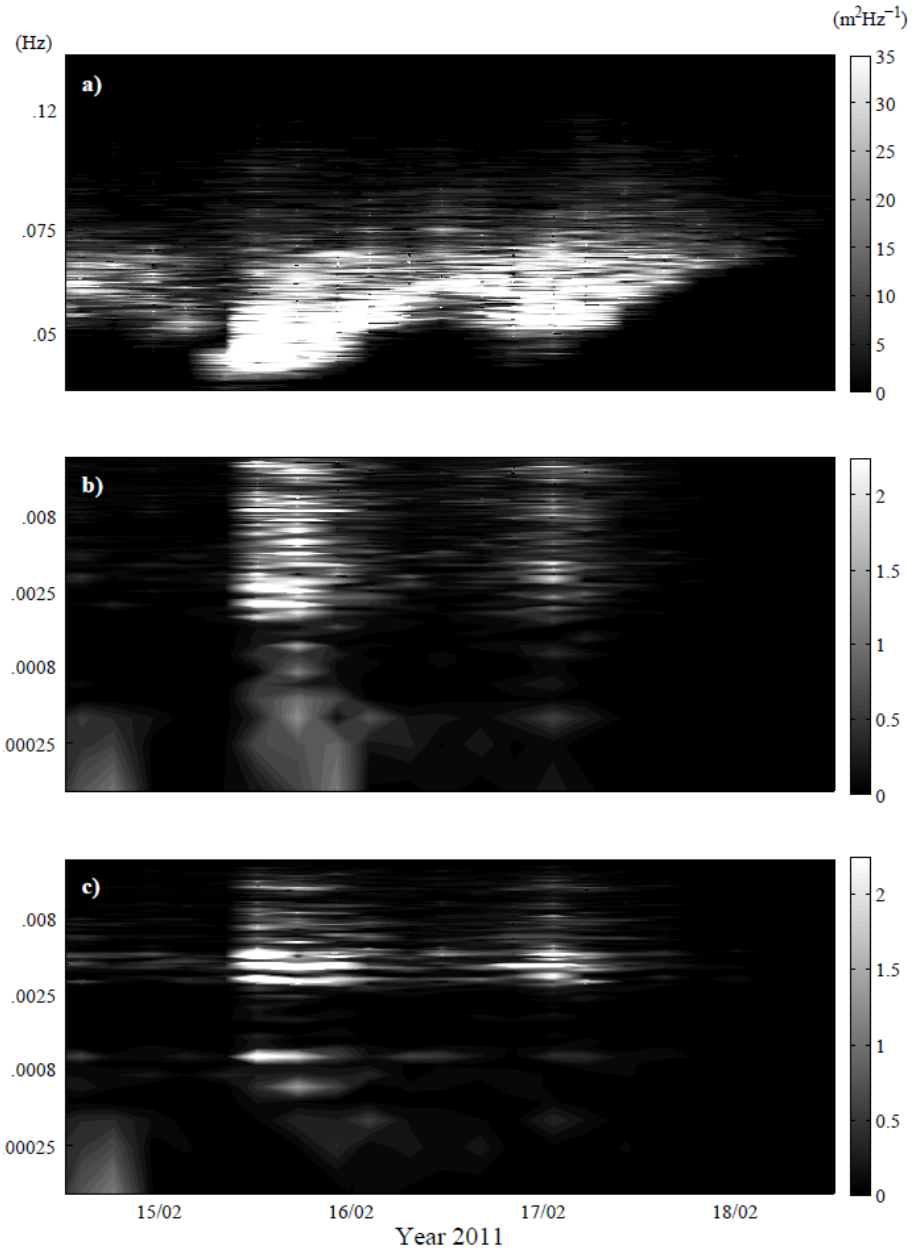

Figure 3. Spectrogram of sea surface elevation records at different locations and frequency bands[a) Outside the Port, swell frequencies; b) outside the port, long wave frequencies; c) inside the port, long wave frequencies].

3.2. Long waves and vessel movements

The values of $Z_{1/3}$ presented high values for the horizontal plane movements, very close to the proposed in the literature for safe work conditions (Elzinga et al., 1992). The averaged spectra of the vessel movements show a multimodal pattern for all DOFs, with peaks in the power distributions at different frequencies. In particular, the movements in the horizontal plane—i.e. sway and surge (translations), and the (rotation)—present higher power levels at the LF band (Figure 4). This suggests a dominant influence of LF band sea level oscillations on these movements.

A correlation analysis was made to determine this influence of the wave conditions inside the port on the vessel movements. The coefficients of correlation between the swell significant wave height (H_{swell}) and the significant vessel motions ($Z_{1/3}$) for sway, surge and yaw were found to be high ($R > 0.55$). On the other hand, the correlations between the LF band significant wave height (H_{LF}) with $Z_{1/3}$ for the same motions were found slightly lower but also high (Figure 5).

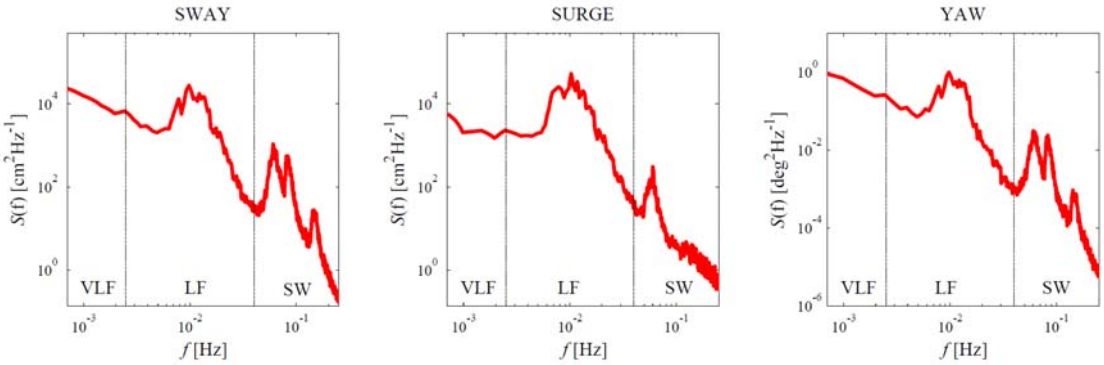

Figure 4. Averaged spectra of the vessel movements in the horizontal plane (sway, surge and yaw).

The latter could suggest a stronger influence of the swell on the vessel movements. However, the vessel motions are positively correlated with the ratio between the LF energy and the total energy; whilst they are negative correlated with the ratio between the swell energy and the total energy. The high correlation between the short wave energy and the energy within the LF band may explain this (Figure 2). In other words, for two sea states with the same energy levels (i.e. the same value of H_s), that one with higher LF energy drives largest vessel movements in the horizontal plane.

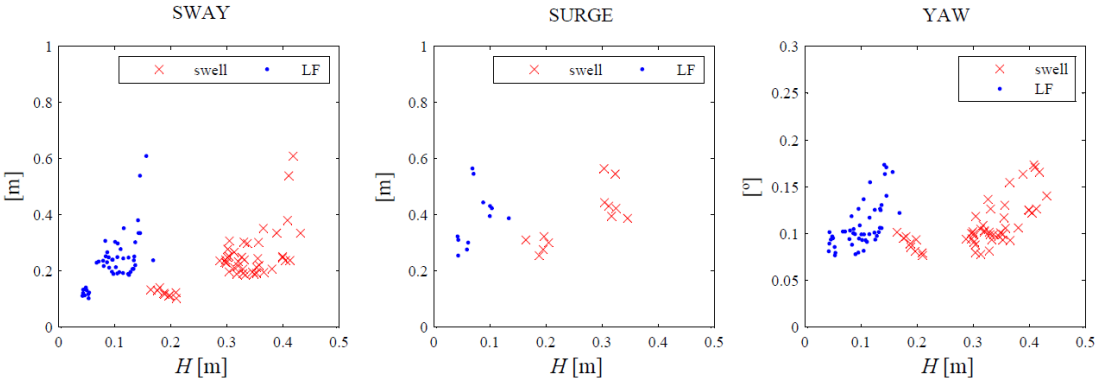

Figure 5. The significant vessel movements ($H_{1/3}$) vs. the LF band and the swell band significant wave heights for the horizontal plane movements (sway, surge and yaw).

3.3. ANN models

An ANN-based model was implemented to determine the LF energy levels inside the port through indirect measurements outside the port. The model takes as inputs the tidal level: d, and the normalized short wave parameters: T_p and H_s (outside the port) and returns as output the significant wave height of the LF band: H_{LF} (inside the port).

A total of 14 different network topologies with one and two hidden layers were compared using the k-fold cross-validation method, with k = 30. The one-hidden-layer topologies selected were: [3-1-1], [3-2-1], [3-3-1], [3-4-1], [3-5-1], [3-6-1], [3-7-1], and [3-8-1]; and the two-hidden-layer topologies were: [3-2-2-1], [3-2-3-1], [3-3-2-1], [3-3-3-1], [3-3-4-1], [3-4-3-1], and [3-4-4-1]. The training and validation errors committed by each topology are shown in Figure 6. Training errors present low and very similar values, indicating a good capability of ANN to learn the problem. As for the validation errors, their values increase with the number of layers and neurons per layer, i.e. with the complexity of the model. The topology minimizing the validation error or best performing topology resulted [3-2-2-1].

After having defined the optimum network topology, the significant LF wave height inside the harbour was predicted for the test data set (Figure 7). The results show a very good agreement between the expected and the computed values, with a correlation coefficient very high ($R > 0.95$) and very low test error (MSE < 4×10^{-4}).

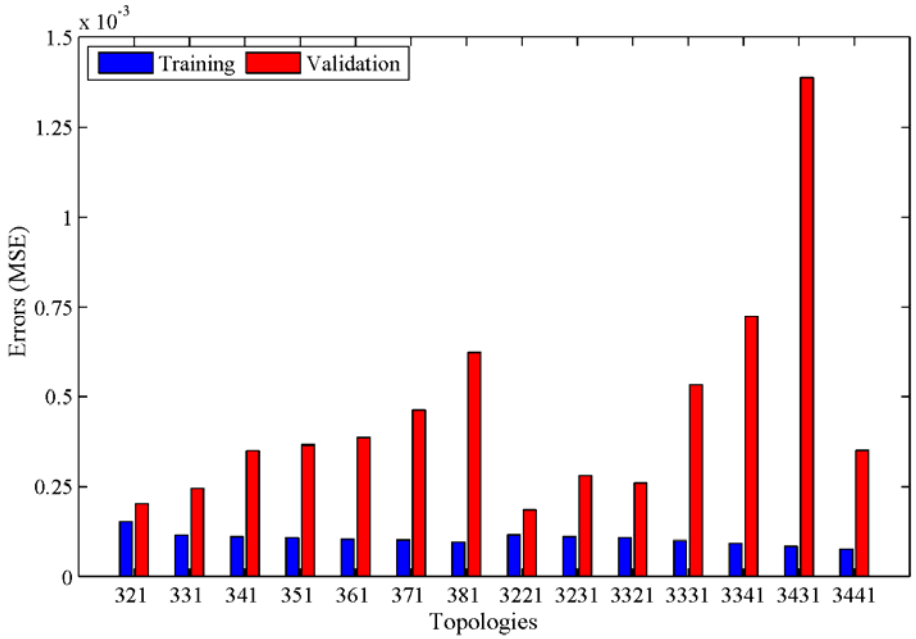

Figure 6. The training, validation and test error for the different ANN topologies compared.

4. CONCLUSIONS

On the basis of the correlation between the swell energy outside the Exterior Port of Ferrol and the long wave energy inside, three frequency bands are proposed: a Low Frequency Band (LF, 2.5 to 40 mHz), highly correlated; a Very Low Frequency band (VLF, 0.7 to 2.5 mHz), with an intermediate correlation; and an Ultra Low Frequency band (ULF, 0.122 to 0.7 mHz), only weakly correlated. The energy levels of the LF band where associated with extreme swell events outside the port, confirming the swell-driven nature of the LF band, which is associated to the so-called infragravity waves.

Once characterized the behaviour and the nature of the long waves in the port, their influence on the movements of a bulk carrier berthed at the port between 19th and 21st February 2011 was studied. The movements in the 6 DOFs (heave, sway, surge, yaw, pitch and roll) were analyzed through frequency and time domain techniques. The horizontal plane movements (sway, surge and yaw) show power distributions dominated by low frequency harmonics within the LF band. Moreover, these movements present a high and positive correlation with the ratio between the LF energy to the total wave energy, indicating a dominant influence of infragravity waves in these vessel movements.

Given the relevance of LF band waves inside the port for the port operations, a method for estimating this energy through Artificial Intelligence was applied. To this end, ANNs were implemented and optimized to compute the significant wave height of the LF band, H_{LF}. The model takes as inputs the short wave parameters outside the port and water depth. Different neural topologies were trained and validate through *k*-fold cross validation and all of them yielded very low training errors. However, important differences in their validation errors were found and, thus, selecting appropriate network topologies should be considered in future applications. Artificial neural networks constitute a valid, efficient approach for estimating wave energy in the infragravity band inside a harbour—an issue of great engineering interest.

In sum, in this work, not only the occurrence of resonant episodes due to long waves at the Port of Ferrol is demonstrated, but also the influence of these oscillations on the movements of a vessel at berth. On these grounds, an ANN model was optimized to and applied to predict the LF energy inside a port basin, which was found to influence the horizontal vessel movements. The results and conclusions drawn provide the basis for a port management system with the long wave conditions integrated. In addition, the methodology employed here can be extrapolated to ports with similar problematic to the Port of Ferrol. New investigations at other ports and for other types of vessels will be of major interest, in order to compare the results with those presented here.

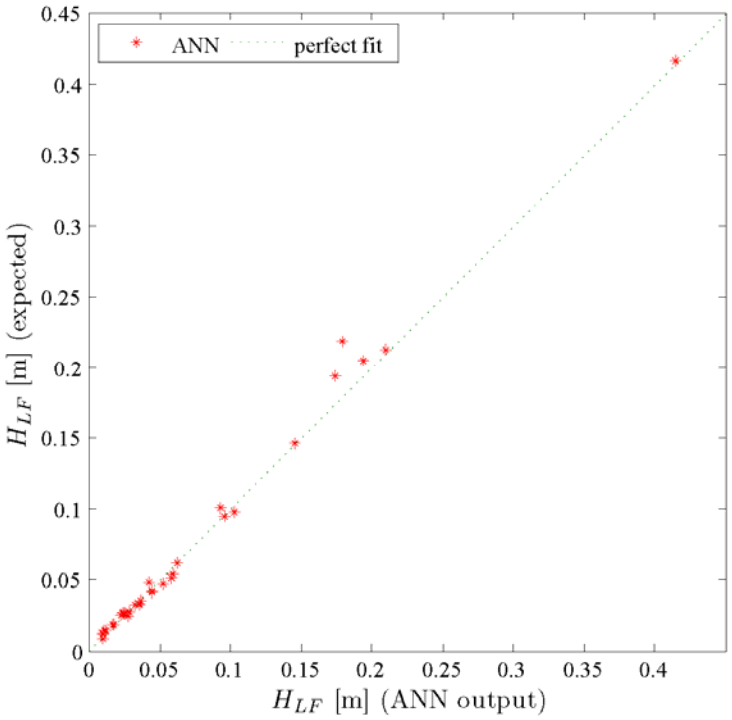

Figure 7. Values expected for of *HLF* vs. values obtained with the ANN.

REFERENCES

Bellotti, G., L. Franco. 2011. Measurement of long waves at the harbor of marina di carrara, Italy. *Ocean Dynamics*, 61(12), 2051-2059.

Candella, R. N. 2009. Meteorologically induced strong seiches observed at Arraial do Cabo, RJ, Brazil. *Physics and Chemistry of the Earth*, 34(17-18), 989-997.

Cecioni, C., G. Bellotti. 2010. Modeling tsunamis generated by submerged landslides using depth integrated equations. *Applied Ocean Research*, 32(3), 343-350.

Elzinga, T., J.R. Iribarren, O.J. Jensen. 1992. Movements of moored ships in harbours. Proceedings of the 23rd International Conference on Coastal Engineering, ASCE, 3216-3229.

Giese, G., D. Chapman, P. Black, J. Fornshell. 1990. Causation of large-amplitude coastals eiches on the Caribbean coast of Puerto Rico. *Journal of Physical Oceanography*, 20(9), 1449-1458.

González-Marco, D., J.P. Sierra, O. Fernández de Ybarra, A. Sánchez-Arcilla. 2008. Implications of long waves in harbor management: The Gijón port case study. *Ocean & Coastal Management*, 51(2), 180-201.

Goring, D.G. 2005. A rissaga nowcasting system. Proceedings of waves 2005 conference, Madrid (pp. 3-7).

Johansson, E. M., F.U. Dowla, D.M. Goodman. 1992. Backpropagation learning for multi-layer feed-forward neural networks using the conjugate gradient method. *International Journal of Neural Systems*, 2(4), 291-301.

Kovalev, P. D., A.B. Rabinovich, G.V. Shevchenko. 1991. Investigation of long waves in the tsunami frequency band on the southwestern shelf of Kamchatka. *Natural Hazards*, 4(2), 141-159.

López, M., G. Iglesias. 2014. Long wave effects on a vessel at berth. *Applied Ocean Research*, 47, 63-72.

López, M., & G. Iglesias. 2013. Artificial Intelligence for estimating infragravity energy in a harbour. *Ocean Engineering*, 57, 56-63.

López, M., G. Iglesias, N. Kobayashi, N. 2012. Long period oscillations and tidal level in the Port of Ferrol. *Applied Ocean Research*, 38, 126-134.

Melito, I., G. Cuomo, L. Franco, R. Guza. 2007. Harbour resonance at Marina di Carrara: Linear and non linear aspects. Proceedings of Coastal Structures, 1647-1658.

Morison, M., J. Imberger. 1992. Water-level oscillations in Esperance Harbour. *Journal of Waterway Port Coastal and Ocean Engineering*, 118(4), 352-367.

Munk, W. 1949. Surf beat. Eos Trans.AGU, 30, 849-854.
Okihiro, M., & Guza, R. T. (1996). Observations of seiche forcing and amplification in three small harbors. Journal of Waterway Port Coastal and Ocean Engineering, 122(5), 232-238.
PIANC. 1995. Criteria for movements of moored ships in harbours: A practical guide. report of working group no. 24 of the permanent technical committee II. Brussels, Belgium: PIANC, General Secretariat.
Rabinovich, A. 2009. Seiches and harbour oscillations. In Y. Kim (Ed.), Handbook of coastal and ocean engineering (pp. 193-236). Singapoure: World Scientific Publishing.
Sakakibara, S., M. Kubo. 2008. Characteristics of low-frequency motions of ships moored inside ports and harbors on the basis of field observations. *Marine Structures*, 21(2), 196-223.
Wilson, B. 1972. Seiches. Advances in Hydroscience, 8, 1-94.